

FIBER BRAGG GRATING SENSORS AS BEAM-INDUCED HEATING MONITOR FOR THE CENTRAL BEAM PIPE OF CMS

F. Fienga^{1,*}, L. Sito¹, V. R. Marrazzo¹, A. Irace, and G. Breglio¹

Univeristy of Naples Federico II, Naples, Italy

F. Carra, F. Giordano, and B. Salvant,

European Organization for Nuclear Research (CERN), Geneva, Switzerland

N. Beni¹, and Z. Szillasi¹,

Institute for Nuclear Research of Eötvös Loránd Research Network, Debrecen, Hungary

S. Buontempo¹, National Institute for Nuclear Physics (INFN), Naples, Italy

¹also at European Organization for Nuclear Research (CERN), Geneva, Switzerland

Abstract

The passage of a high-intensity particle beam inside accelerator components generates heating, potentially leading to degradation of the accelerator performance or damage to the component itself. It is therefore essential to monitor such beam-induced heating in accelerators. This paper showcases the capabilities of iPipe, which is a set of Fiber Bragg Grating sensors stuck on the inner beam pipe of the Compact Muon Solenoid (CMS) experiment installed in the CERN Large Hadron Collider (LHC). In this study, the wavelength shift, linked directly to the temperature shift, is measured and is compared with the computed dissipated power for a set of LHC fills. Electromagnetic and thermal simulations were also coupled to predict the beam-induced temperature increase along the beam pipe. These results further validate the sensing system and the methods used to design accelerator components to mitigate beam-induced heating.

INTRODUCTION

An increase in energy and intensity of the beams is expected as part of the CERN's Large Hadron Collider (LHC) High Luminosity (HL) upgrade [1]. One of the major potential limitations for this upgrade [2] is the heating of accelerator components produced by the presence of the beam itself. This is called beam-induced heating (BIH).

The beam-induced heat load is deposited on the device primarily in three ways: (i) synchrotron radiation [3], (ii) electron cloud [4], and (iii) heating due to impedance [5].

These phenomena can lead to several issues (delays, beam dumps, and even component damage) like, for instance, what occurred in June 2011 during the first Run of LHC [6]. Therefore, it is essential that the components' design phase is able to appropriately account for heating. Additionally, it is necessary to have suitable monitoring systems to regularly monitor temperature-related parameters.

One sensing solution that has spread in the last decade in the High Energy Physics domain is Fiber Optic Sensing (FOS). This work focuses on iPipe, an innovative measuring system based on Fiber Bragg Gratings (FBGs), mounted

in the CMS experiment and in acquisition since 2015 [7]. The iPipe system is monitoring CMS's vacuum chamber, the Central Beam Pipe (CBP). Since the CBP is located at one of the interaction points, it is hosting both beams simultaneously to allow them to collide. This two counter-rotating beams situation causes interference phenomena that can lead to an anomalous dissipated power distribution [5].

The possibility to infer various beam parameters using data logged by the iPipe system has already been demonstrated [8]. This work aims to go further, comparing the temperature excursion acquired by the iPipe system during machine operation with a temperature map produced using coupled electromagnetic and thermal simulations. The main goal is to demonstrate the capability of the iPipe system to measure directly the BIH. Moreover, this benchmark enables to further validate the analytical model (with regards to the two counter-rotating beams case in particular) and simulation methodologies that are typically used at CERN.

MEASUREMENTS

FBGs are periodic changes in the refractive index of the optical fiber's core. Such a structure behaves as a stop band filter: it reflects light centered at a specific wavelength, that is called Bragg wavelength (λ_B), and that depends on the effective refractive index of the core (n_{eff}) and the spatial periodicity of the grating (Λ). These dependencies are described in Eq. (1).

$$\lambda_B = 2n_{eff}\Lambda. \quad (1)$$

This structure is intrinsically a sensor since any change either in the refractive index of the core or in the grating period results in a change of the Bragg wavelength. A temperature difference (ΔT) and/or an applied strain (ε) may cause these changes and, as described by Eq. (2), it is possible to correlate the superposition of the two physical effects with the Bragg wavelength variation that they induce [9].

$$\Delta\lambda_B(T, \varepsilon) = \lambda_B \cdot [(1 - \rho_e) \cdot \varepsilon + (\alpha_\Lambda + \alpha_n) \cdot \Delta T], \quad (2)$$

where ρ_e is the photo-elastic effect coefficient, α_Λ is the thermal expansion coefficient, and α_n is the thermo-optic effect coefficient.

* francesco.fienga@unina.it

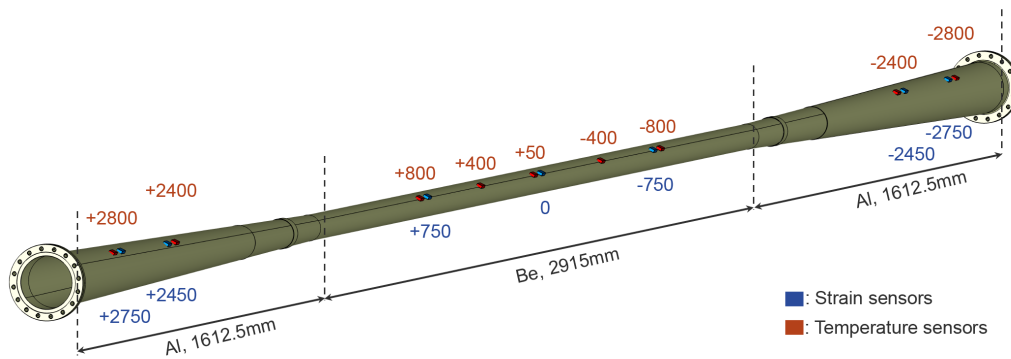


Figure 1: 3D CAD model of the CBP during Run2 (2015-2018). The probes' names refer to their distance from the IP in mm.

Placing the probe only in thermal contact with the structure, thus applying ideally no strain on the fiber, allows to measure the temperature alone. However, during the mounting phase, a certain amount of strain will always be induced. It is then more practical to talk about a wavelength variation, directly linked to a temperature variation, to filter out the initially induced strain.

This approach of relative measurements can be advantageous also in terms of radiation hardening of the FBGs. An ionizing radiation could affect the FBG with a radiation-induced Bragg wavelength shift (RI-BWS). In the case of iPipe, the FBGs employed are femtosecond laser inscribed (fFBG) and this guarantees already a suitable radiation hardening of the probes for the considered environment [10]. Moreover, the dose rate in LHC is such that impact of radiation on the measurements is completely negligible when considering the difference in wavelength.

The case study is the beam pipe of CMS. During the Run2 of LHC (2015-2018) it was made of a central cylindrical section of beryllium, with an external diameter of 45 mm, a thickness of 0.8 mm and a length of almost 3 m. Two conical aluminium sections are then sealing the central region. A 3D CAD model of the structure, with a schematic representation of the probes' position, can be seen in Fig. 1.

The iPipe system is composed of 4 arrays (i.e. 4 optical fibers; only one array is shown in Fig. 1) each with 16 FBG sensors: 7 are glued to the structure to measure strain, 9 are only in thermal contact with the surface to measure temperature variations [7]. In this work the strain probes will not be considered. Moreover, only the central cylindrical section is considered for simplicity. All the results presented in this proceeding are referring to the sensor named P50, that is placed at 50 mm from the beams' collision point, also called Interaction Point (IP).

In Fig. 2, the Bragg wavelength - measured by interrogating the iPipe probe (green curve) - is reported in its evolution in time during the LHC fill 6675 (12-13 May 2018). Moreover, the intensities of the two beams (red and blue curves are respectively beam 1 and beam 2 intensities) are reported. One can observe that the wavelength shift is correlated to

the intensity curve with an initial delay. Furthermore, it is interesting to notice the change in concavity of the curve at the end of the intensity ramp. After further investigations it was possible to conclude that the second temperature increase, is due to additional heating coming from the silicon trackers placed all around the CBP that are being turned on.

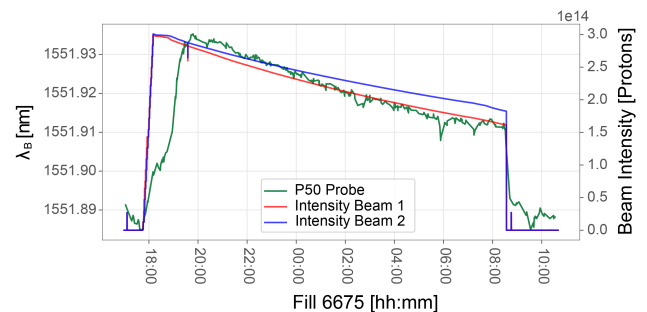


Figure 2: Evolution of the Bragg wavelength measured by the P50 probe during the fill 6675 (green curve). Evolution of the intensity of beam 1 (red) and beam 2 (blue).

This is a showcase of the capabilities of the sensing system that has proven to be an effective solution to monitor the temperature variations continuously at multiple locations along the CMS beam pipe. In particular some peculiarities make it more attractive than other solutions for the CMS environment: (i) multiplexing capabilities and easiness of installation due to the reduced cabling, (ii) immunity to electromagnetic interference (EMI), (iii) robustness to ionizing radiation, and (iv) reduced probability of interacting with generated sub-particles due to the small diameter of the fiber (200 μm).

SIMULATIONS

To effectively produce a temperature map, the approach considered consists of two phases: (i) computing the dissipated power distribution due to the passage of the beam into the component, then (ii) using the power distribution, together with the appropriate thermal boundary conditions and symmetries of the problem, as input for a thermal solver.

Content from this work may be used under the terms of the CC BY 4.0 licence (© 2022). Any distribution of this work must maintain attribution to the author(s), title of the work, publisher, and DOI

Electromagnetic Simulations

In the considered case, two counter-rotating beams are circulating in the component at the same time. This leads to interference phenomena and to a dissipated power distribution that depends on the distance from the IP. The analytical relation of the dissipated power in the two beams case, for a symmetrical beam chamber, is reported in [5]. The actual relation that was employed, after having applied the appropriate simplifications, is presented in Eq. (3).

$$\Delta W(s) = (2f_0 e N_{beam})^2 \sum_{p=0}^{\infty} |\Lambda(p\omega_0)|^2 \cdot \text{Re}[Z(p\omega_0)] \cdot (1 - \cos(p\omega_0\tau_s)), \quad (3)$$

where, $f_0 = \frac{\omega_0}{2\pi}$ is the revolution frequency of the beam, e is the charge of the particle, N_{beam} is the number of particles in the beam, Λ is the normalized beam spectrum, Z is the longitudinal beam coupling impedance, and $\tau_s = \frac{2s}{c}$ is the phase shift, with s the distance from the IP and c the speed of light in vacuum.

To effectively implement the equation, the procedure shown in Fig. 3 was used. It is a completely general procedure, that enables to study the dissipated power in a given accelerator component. Starting from the geometry of the device and its material, it is possible to compute the longitudinal beam-coupling impedance.

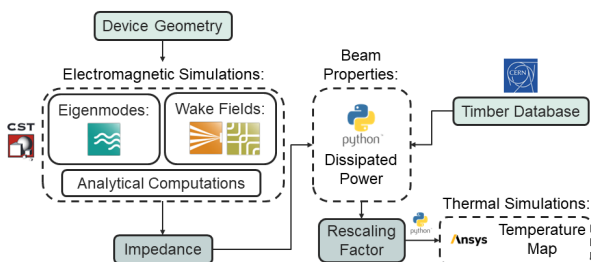


Figure 3: Schematic description of the procedure adopted for electromagnetic simulations.

A python tool was developed to access the CERN's database Timber to extract the parameters of the beams during a certain fill of LHC. This information allows computing the dissipated power density distribution along the structure, as shown in Fig. 4. The dissipated power density distribution (violet curve) is reported as a function of the phase shift (i.e. the distance from the IP) for fill 6675. In addition, the single beam power loss density is shown to underline the overshoot due to the two-beam interactions. Finally, on top of the graph, one half of the CBP is shown with the IP and the positions of the probes highlighted.

Thermal Simulation

Once the dissipated power distribution along the beam pipe has been calculated, it is possible to use it as excitation for a thermal simulation in ANSYS. In addition, to perform the simulation, it is necessary to model the thermal

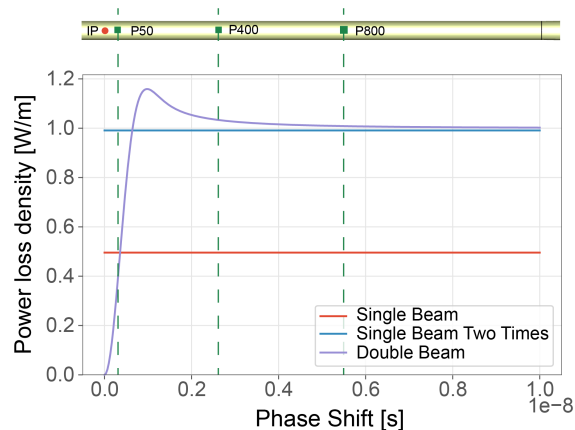


Figure 4: Dissipated power distribution along one half of the CBP for two beams case (violet), single beam case (red), and two times the single beam case (blue).

boundary conditions of the problem accurately. The CBP is surrounded by particle trackers: the closest are the Barrel Pixel Tracker (BPIX) and the Forward Pixel Tracker (FPix). These trackers are operating at a nominal temperature of -22°C therefore, they are contained in two service cylinders that bring electrical connections and cooling system. Moreover, to avoid air condensation, a dry air inlet of $3\text{ m}^3/\text{h}$ is provided through a series of holes on top of the BPIX. This whole system described is isolated from the remaining cavern with a thermal jacket [11]. The problem was simplified to obtain the film coefficients along the beam pipe through the use of empirical relations. The value of the analytically calculated coefficients is then reduced in the last portion of the central pipe to take into account: (i) the degradation of the heat exchange mechanism, (ii) the dissipated power coming from the conical sections. The film coefficients applied to the structure are summarized in Table 1.

Table 1: Film coefficient profile along the CBP. The reference point is the IP.

Longitudinal position	Local Film Coeff.
0–274.4 mm	0.655 W/m ² K
274.4–515 mm	3.34 W/m ² K
515–1500 mm	1.20 W/m ² K

RESULTS

Results from the electromagnetic simulation alone will be presented first and then, the result of the final thermal benchmark will be discussed.

For each fill of 2018, thanks to the procedure shown in the electromagnetic simulations section, it was possible to compute the local dissipated power density at 50 mm from the IP and compare it with the temperature excursion registered by the iPipe P50 probe. To get a more significant result, the 2018 fills were filtered to keep only the ones with:

(i) declared stable beam phase, (ii) total duration longer than 6 hr, and (iii) number of bunches greater than 300. After this process, of all the fills of 2018, in Fig. 5, 89 are shown. In addition, a color-map is present as an indication of the maximum intensity of the fill.

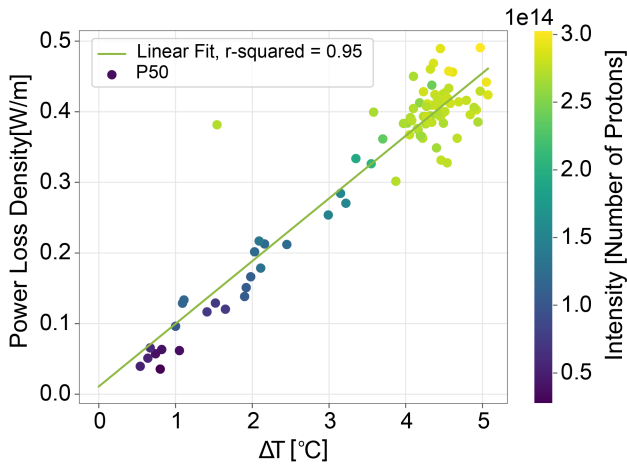


Figure 5: Simulated local dissipated Power against measured temperature excursion.

The data were fitted showing an excellent linearity, with an r-squared of 0.95. This represents an important result that demonstrates the possibility of directly assessing BIH with optical fiber temperature measurements.

A further validation comes from a thermal simulation performed on a subset of 10 fills. The selected fills occurred between April and May 2018 and represent extremely controlled situations. Having computed the dissipated power distribution along the CBP, with the assumption of distributing radially the local dissipated power, the heat source can be considered known. After applying the appropriate symmetries and boundary conditions of the problem, it was possible to obtain a temperature map with ANSYS. For these 10 fills, the thermal excursion registered by the iPipe sensors is compared with the thermal excursion obtained by simulation. The results are shown in Fig. 6 and the agreement is excellent considering the complexity of the problem and the number of approximations made.

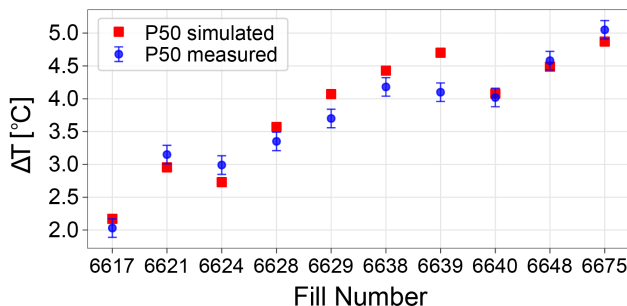


Figure 6: Comparison of simulated and measured temperature excursions.

CONCLUSION

The major purpose of this study has been to validate further the usage of FOS sensing, and more specifically the FBG technology, for monitoring particle accelerator components. It was shown that the iPipe system enables to measure directly the dissipated power due to the passage of the beam. Moreover, a further validation of both the sensing technology and the accelerator component design methodologies was given thanks to a coupled electromagnetic and thermal simulation.

ACKNOWLEDGEMENTS

The authors would like to thank N. Bacchetta, A. Filenius, J. Guardia Valenzuela, M. Masci, G. Rumolo, C. Zannini, and W. Zeuner for their contribution.

REFERENCES

- [1] G. Apollinari, O. Brüning, T. Nakamoto, and L. Rossi, “High Luminosity Large Hadron Collider HL-LHC”, 2015. doi: 10.5170/CERN-2015-005.1
- [2] G. Arduini *et al.*, “High Luminosity LHC: challenges and plans”, *J. Instrum.*, vol. 11, p. C12081, 2016. doi: 10.1088/1748-0221/11/12/C12081
- [3] A. A. Sokolov and I. M. Ternov, *Synchrotron radiation*. Akademie-Verlag Berlin, Germany; Pergamon Press, Oxford and cop. 1968.
- [4] G. Rumolo *et al.*, “Electron cloud effects on beam evolution in a circular accelerator”, *Phys. Rev. ST Accel. Beams*, vol. 6, p. 081002, 2003. doi: 10.1103/PhysRevSTAB.6.081002
- [5] C. Zannini, G. Iadarola, and G. Rumolo, “Power Loss Calculation in Separated and Common Beam Chambers of the LHC”, in *Proc. IPAC’14*, Dresden, Germany, Jun. 2014, pp. 1711–1713. doi: 10.18429/JACoW-IPAC2014-TUPRI061
- [6] B. Salvant *et al.*, “Update on Beam Induced RF Heating in the LHC”, in *Proc. IPAC’13*, Shanghai, China, May 2013, paper TUPME032, pp. 1646–1648.
- [7] F. Fienga *et al.*, “A fiber optic sensors monitoring system for the central beam pipe of the CMS experiment”, *Opt. Laser Technol.*, vol. 120, p. 105650, 2019. doi: 10.1016/j.optlastec.2019.105650
- [8] F. Fienga *et al.*, “Fiber Bragg Grating Sensors as Innovative Monitoring Tool for Beam Induced RF Heating on LHC Beam Pipe”, *J. Lightwave Technol.*, vol. 39, pp. 4145–4150, 2021. doi: 10.1109/JLT.2021.3062458
- [9] K. O. Hill and G. Meltz, “Fiber Bragg grating technology fundamentals and overview”, *J. Lightwave Technol.*, vol. 15, pp. 1263–1276, 1997. doi: 10.1109/50.618320
- [10] A. Gusarov and S. K. Hoeffgen, “Radiation Effects on Fiber Gratings”, *IEEE Trans. Nucl. Sci.*, vol. 60, pp. 2037–2053, 2013. doi: 10.1109/TNS.2013.2252366
- [11] CMS Collaboration *et al.*, “The CMS experiment at the CERN LHC”, *J. Instrum.*, vol. 3, 2008. doi: 10.1088/1748-0221/3/08/S08004